

Conservation and Divergence of Circadian Clock Operation in a Stress-Inducible Crassulacean Acid Metabolism Species Reveals Clock Compensation against Stress¹

Susanna F. Boxall, Jonathan M. Foster, Hans J. Bohnert², John C. Cushman, Hugh G. Nimmo, and James Hartwell*

Department of Biology, University of York, York YO10 5YW, United Kingdom (S.F.B., J.M.F., J.H.); Division of Biochemistry and Molecular Biology, Institute of Biomedical and Life Sciences, University of Glasgow, Glasgow G12 8QQ, United Kingdom (H.G.N.); Department of Biochemistry and Molecular Biophysics, University of Arizona, Tucson, Arizona 85721 (H.J.B.); and Department of Biochemistry, University of Nevada, Reno, Nevada 89557 (J.C.C.)

One of the best-characterized physiological rhythms in plants is the circadian rhythm of CO₂ metabolism in Crassulacean acid metabolism (CAM) plants, which is the focus here. The central components of the plant circadian clock have been studied in detail only in *Arabidopsis* (*Arabidopsis thaliana*). Full-length cDNAs have been obtained encoding orthologs of *CIRCADIAN CLOCK-ASSOCIATED1* (*CCA1*)/*LATE ELONGATED HYPOCOTYL* (*LHY*), *TIMING OF CAB EXPRESSION1* (*TOC1*), *EARLY FLOWERING4* (*ELF4*), *ZEITLUPE* (*ZTL*), *FLAVIN-BINDING KELCH REPEAT F-BOX1* (*FKF1*), *EARLY FLOWERING3* (*ELF3*), and a partial cDNA encoding *GIGANTEA* in the model stress-inducible CAM plant, *Mesembryanthemum crystallinum* (Common Ice Plant). *TOC1* and *LHY/CCA1* are under reciprocal circadian control in a manner similar to their regulation in *Arabidopsis*. *ELF4*, *FKF1*, *ZTL*, *GIGANTEA*, and *ELF3* are under circadian control in C₃ and CAM leaves. *ELF4* transcripts peak in the evening and are unaffected by CAM induction. *FKF1* shows an abrupt transcript peak 3 h before subjective dusk. *ELF3* transcripts appear in the evening, consistent with their role in gating light input to the circadian clock. Intriguingly, *ZTL* transcripts do not oscillate in *Arabidopsis*, but do in *M. crystallinum*. The transcript abundance of the clock-associated genes in *M. crystallinum* is largely unaffected by development and salt stress, revealing compensation of the central circadian clock against development and abiotic stress in addition to the well-known temperature compensation. Importantly, the clock in *M. crystallinum* is very similar to that in *Arabidopsis*, indicating that such a clock could control CAM without requiring additional components of the central oscillator or a novel CAM oscillator.

In higher plants, a circadian clock controls hypocotyl elongation, daily leaf movements, flowering time, and the rhythm of CO₂ fixation in Crassulacean acid metabolism (CAM; McClung, 2001). Some of the molecular components of the central plant clock have been identified. The closely related single Myb-repeat transcription factors, termed *CIRCADIAN CLOCK-ASSOCIATED1* (*CCA1*) and *LATE ELONGATED HYPOCOTYL* (*LHY*), and the pseudoresponse regulator/CONSTANS-motif protein, *TIMING OF CAB*

EXPRESSION1 (*TOC1*), form at least part of the central clock (Eriksson and Millar, 2003). *CCA1* and *LHY* are expressed around dawn when they bind to the promoter of *TOC1* and repress its expression (Alabadi et al., 2001). As dusk approaches, the levels of *CCA1* and *LHY* decrease, *TOC1* expression is derepressed, and *TOC1* is expressed during the evening. *TOC1* is thought to act as a positive element in the regulation of *CCA1* and *LHY*, but it is clear that this occurs in concert with the action of other genes. Candidates for genes that act in concert with *TOC1* to induce *CCA1* and *LHY* include *EARLY FLOWERING3* (*ELF3*), *GIGANTEA* (*GI*), and *EARLY FLOWERING4* (*ELF4*; Doyle et al., 2002; Eriksson and Millar, 2003).

A number of other genes have been implicated in the *Arabidopsis* (*Arabidopsis thaliana*) clock. *ELF3* is a novel protein that has been shown to gate light input to the clock (McWatters et al., 2000). When *ELF3* is expressed in the evening, light input to reset the clock is blocked. The *ZEITLUPE* (*ZTL*) family of proteins, *ZTL*, *FLAVIN-BINDING KELCH REPEAT F-BOX1* (*FKF1*), and *LIGHT, OXYGEN OR VOLTAGE* (*LOV*), *KELCH PROTEIN2* (*LKP2*), have all been shown to play a role in circadian clock function. An *Arabidopsis* 35S::*LKP2* overexpress-

¹ This work was supported by a Biotechnology and Biological Sciences Research Council, UK, David Phillips Fellowship (grant no. JF14818 to J.H.), and in part by the National Science Foundation (grant no. DBI-9813360 to H.J.B.). J.C.C. acknowledges support from the National Science Foundation (grant nos. IBN-0196070 and DBI-9813360) and the Nevada Agricultural Experiment Station (publication no. 03043029).

² Present address: Department of Plant Biology, University of Illinois, Urbana, IL 61801.

* Corresponding author; e-mail jh54@york.ac.uk; fax 44-1904-328762.

Article, publication date, and citation information can be found at www.plantphysiol.org/cgi/doi/10.1104/pp.104.054577.

ing line has arrhythmic clock output in several circadian rhythms (Schultz et al., 2001). *ztl* is a long-period mutant, whereas *fkf1* is a late-flowering mutant in long days and has subtle defects in circadian control of gene expression (Nelson et al., 2000; Somers et al., 2000). Unlike *ZTL*, *FKF1* does not affect circadian period and has been demonstrated to act downstream of the clock to control the photoperiodic switch to flowering (Imaizumi et al., 2003). The *FKF1* LOV domain can bind to a flavin mononucleotide chromophore and undergo light-induced photochemistry, suggesting that *FKF1* could directly sense blue light (Imaizumi et al., 2003). *ZTL* has recently been shown to interact directly with *TOC1* and target it for degradation via a proteasome-dependent pathway (Mas et al., 2003). Furthermore, the abundance of the *ZTL* protein itself is under circadian control with the turnover involving the proteasome, and *ZTL* forms part of an SCF complex in vivo (Kim et al., 2003; Han et al., 2004).

The physiology and biochemistry of the circadian rhythm of CAM CO₂ fixation is relatively well characterized (Wilkins, 1992; Lüttge, 2000, 2003). Phosphoenolpyruvate carboxylase (PEPc) catalyzes primary CO₂ fixation in CAM plants. PEPc is activated at night by a phosphorylation event that is driven by a circadian clock. Circadian oscillations in the phosphorylation state of PEPc are due to circadian control of the expression and activity of PEPc kinase (PPCK; Carter et al., 1991; Hartwell et al., 1996, 1999, 2002). Phosphorylation reduces the sensitivity of PEPc to feedback inhibition by malate, and this makes phospho-PEPc more active in vivo at night, allowing malate to accumulate in the vacuole. Interestingly, the circadian control of the CAM pathway and *PPCK* expression and activity can be overridden by metabolic perturbations that influence the subcellular localization of malate (Borland et al., 1999).

We have a far more limited knowledge of the molecular machinery that underlies the CAM CO₂ rhythms. One proposal considers that the movement of malate into and out of the vacuole, with the tonoplast functioning as a discrete hysteresis switch, could itself form the basis of the CAM circadian oscillator (Wilkins, 1992; Lüttge, 2000, 2003). Computer modeling of this biophysical oscillator has demonstrated that it could sustain robust rhythmicity of CAM over a range of temperatures (Lüttge, 2000). However, Wyka et al. (2004) found that preventing nocturnal malate accumulation in *Kalanchoë daigremontiana* did not cause the predicted phase delays generated by the aforementioned computer model. The authors conclude that their results rule out vacuolar malic acid accumulation as the central pacemaking process in *Kalanchoë* (Wyka et al., 2004). The current paradigm is that the central circadian oscillator responsible for all rhythmic outputs consists of a discrete suite of genes, which form an autoregulatory negative feedback loop. A testable hypothesis assumes that a similar clock could provide the circadian control of the CAM pathway and that the movement of malate in and out of the vacuole responds

to a molecular clock. Conversely, the metabolic signals provided by the operation of CAM (e.g. high cytosolic malate during the day or high starch at dusk) could be involved in entraining the central clock genes or in modulating the output pathways from the clock. To test these hypotheses, we have identified orthologs of the molecular components of the plant circadian oscillator from the model plant, *Mesembryanthemum crystallinum* (Common Ice Plant), in which CAM is inducible. These genes allow us to address fundamental questions about the molecular basis of the circadian control of the CAM pathway.

We report the cloning and characterization of orthologs of seven Arabidopsis circadian clock-associated genes from *M. crystallinum*, hereafter referred to as *McCCA1/McLHY*, *McTOC1*, *McELF4*, *McZTL*, *McFKF1*, *McGI*, and *McELF3*. Here, we characterize all of these clock-associated genes in a plant species other than Arabidopsis and, importantly, we demonstrate central clock operation in a CAM species. We identify *McZTL* as a clock-associated gene whose regulation has changed during the divergence of *M. crystallinum* and Arabidopsis from a common ancestor. Also, it is established that the central clock operates robustly throughout development, regardless of stress conditions.

RESULTS

Identification of Central Circadian Clock Genes in *M. crystallinum*

Database searches using the TBLASTN search algorithm against the *M. crystallinum* gene index of expressed sequence tags (ESTs; Kore-eda et al., 2004) revealed EST sequences with similarity to *AtCCA1/AtLHY*, *AtELF4*, *AtZTL*, *AtGI*, and *AtELF3*. We used these EST sequences to design the reverse transcription (RT)-PCR primers in Table I that specifically target the *M. crystallinum* orthologs of these genes. The RT-PCR products were cloned and sequenced to confirm that the amplified product was gene specific. We also cloned a fragment of *McZTL* and *McFKF1* via degenerate PCR, using primers to the conserved domains of plant *ZTL* family proteins (see "Materials and Methods"). A fragment of the *McTOC1* gene was isolated using primers specific to sugar beet (*Beta vulgaris*) EST sequences (GenBank accession nos. BI543444 and BI543434), with high similarity to *AtTOC1*. As a member of the order Caryophyllales, sugar beet is in the same taxonomic order as *M. crystallinum*. We reasoned, therefore, that there was a strong likelihood that the *McTOC1* gene would be closely related to the sugar beet *TOC1* gene. The identity of the resulting 300-bp *McTOC1* PCR fragment was confirmed by cloning and sequencing.

Based on the EST and PCR fragment sequences corresponding to each gene, sequence-specific primers were designed for 5' and 3' RACE-PCR of the cor-

Table 1. Primers used for RT-PCR analyses and cloning

Primers with "F" at end of name are forward; primers with "R" at end of name are reverse.

Primer Name	Sequence	Product Size bp	Optimal Cycle No.
McCCA1/LHYF	5'-GCAAAATGCAACAGAAACCA-3'	350	22
McCCA1/LHYR	5'-ATACTTGCTGTGGCCAAGGT-3'		
McTOC1F	5'-TTCATTGATCGAAGTAAAGTCAG-3'	300	28
McTOC1R	5'-CCAGCCTCAAGCACTTTACA-3'		
McELF4F	5'-ATGTGGCGATCATTGAGGA-3'	199	25
McELF4R	5'-CCCTTCATATTCAATCCACCA-3'		
McZTLF	5'-GTGTGGCGAGAATTCCAGT-3'	350	25
McZTLR	5'-TCCTCAGTTGGGTCAAGAAGA-3'		
McFKF1F	5'-GCAAACCTTAGGTGGCTGACC-3'	400	25
McFKF1R	5'-CGGCTTGGAGAGAGATTCTCT-3'		
McGIF	5'-ATCCCCCACTCACCATAACA-3'	302	29
McGIR	5'-GCAAGAGGGCAAATATCCA-3'		
McELF3F	5'-CTCGTAGAGAAGGCGAGCTG-3'	426	25
McELF3R	5'-ACACAAGGCTCCAGCAAGAT-3'		
McCAB2F	5'-TCGCCATCCTACCTTACCG-3'	849	18
McCAB2R	5'-TCATTCATTGGCAACAACG-3'		
McCCR1/2F	5'-ATTCGGCAGGATTTCAAT-3'	315	26
McCCR1/2R	5'-CTCGTTGACGGTGATTTGAC-3'		
McPPCKF	5'-TCTACTCAGGCAAGGGATTTG-3'	699	19
McPPCKR	5'-GAACAAGAACTGGCCAGAA-3'		
McUBQF	5'-TGTTGCATGGTCTGGTTGT-3'	211	18
McUBQR	5'-CGGAAAGAAAACCTTGATTAC-3'		

responding full-length cDNAs. The 3' sequences of *McCCA1/LHY*, *McZTL*, and *McELF3* were obtained by completing the sequence of existing partial cDNAs. The 5' end of the clock genes was amplified from cDNA synthesized using mRNA known to possess each transcript at high abundance (Figs. 2–4). Similarly, the 3' ends of *McTOC1*, *McELF4*, and *McFKF1* were amplified. The RACE-PCR products were either TOPO cloned and sequenced to confirm the identity of the corresponding full-length cDNA sequences for each gene or sequenced directly by primer walking (*McCCA1/LHY*).

Confirmation of Clock Gene Identity

To confirm that we had cloned bona fide *M. crystallinum* orthologs of the Arabidopsis clock genes, we performed multiple sequence alignments between the *M. crystallinum* sequences and the confirmed sequences for the corresponding Arabidopsis genes. We also included the available annotated full-length rice (*Oryza sativa*) orthologs of each clock gene (deduced from the rice genome sequence and The Institute for Genomic Research [TIGR] rice gene index) in the multiple alignments, plus a number of other full-length orthologs identified as tentative consensus (TC) sequences in the TIGR plant gene indexes. Phylogenetic trees generated using the Vector NTI suite AlignX program confirmed the identity of all *M. crystallinum* clock genes (Fig. 1). *McCCA1/McLHY* (AY371287) shows a high degree of similarity with *AtCCA1* (37.5% identity) and *AtLHY* (42.7% identity), particularly in

the single Myb repeat at the N terminus. Specifically, the Myb repeat of *McCCA1/LHY* shares 82.2% identity with *AtLHY* and 83.2% identity with *AtCCA1*. The phylogenetic tree demonstrates that *McCCA1/LHY* is most closely related to the *VvCCA1/LHY* gene from *Vitis vinifera* and that both of these sequences are embedded on a branch of the tree that includes the *PvCCA1/LHY* gene from *Phaseolus vulgaris* (AJ420902; Kaldis et al., 2003; Fig. 1A). The tree does not resolve whether *McCCA1/LHY* is most closely related to *AtCCA1* or *AtLHY*; hence, we maintained its dual name. However, the tree does reveal that the available full-length monocot *CCA1/LHY* sequences from rice (*OsCCA1/LHY* and *OsCCA1/LHY2*), sugarcane (*Saccharum officinarum* [*SoCCA1/LHY*]), and barley (*Hordeum vulgare* [*HvCCA1/LHY*]) are most closely related to *AtCCA1*, suggesting that the rice gene, which has been named *OsLHY* elsewhere (Izawa et al., 2003), might be termed *OsCCA1*. At present, we have not detected a rice *LHY* ortholog in the publicly available rice genome and EST databases.

Casein kinase II can phosphorylate *AtCCA1* and *AtLHY* in vitro and is necessary for its circadian oscillator function (Daniel et al., 2004). Using mass spectrometry, these authors have determined that S-5 and S-6 plus 1 or more of S-431, S-432, S-433, and S-484 are phosphorylated by CK2. These sites are conserved in *McCCA1/LHY*.

The phylogenetic tree based on the alignment of the *McTOC1* gene (AY371288) with the family of 5 Arabidopsis pseudoresponse regulator genes confirms that we have identified a *M. crystallinum* gene that is most

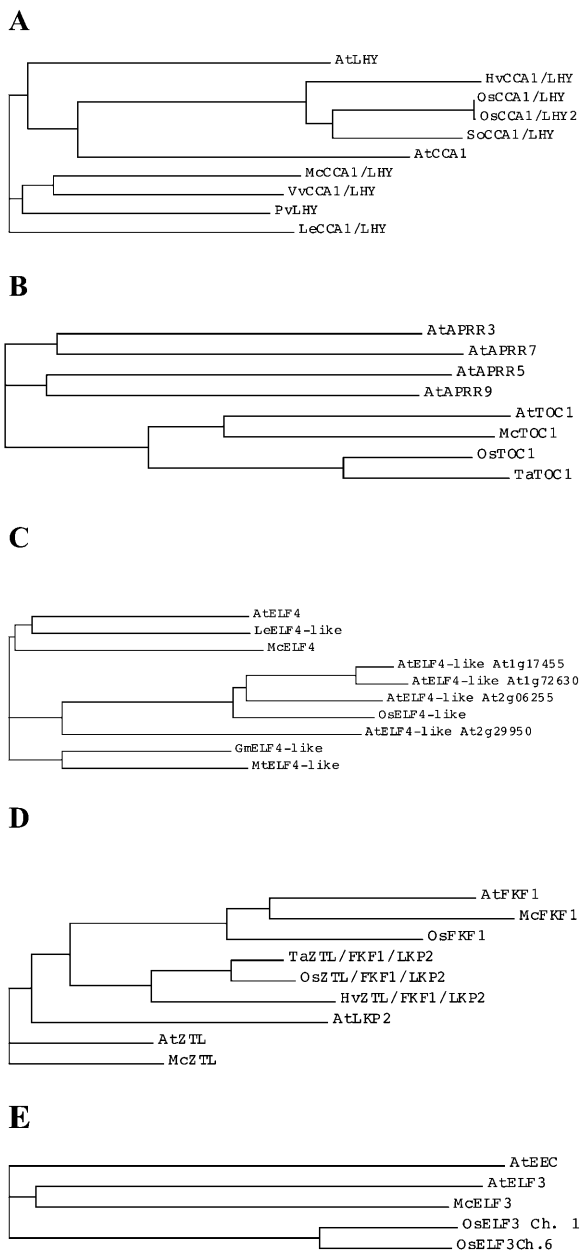


Figure 1. Phylogenetic tree analysis reveals that the *M. crystallinum* clock genes are the orthologs of the Arabidopsis clock genes. A, *McCCA1/LHY* tree. *McCCA1/LHY* (GenBank accession no. AY371287), *AtCCA1* (U28422), *AtLHY* (AJ006404), *PvLHY* (common bean, AJ420902), *LeCCA1/LHY* (tomato, BT012912), *VvCCA1/LHY* (grape, TIGR TC32028), *HvCCA1/LHY* (barley, TC121173), *SoCCA1/LHY* (sugarcane, TC13152), *OsCCA1/LHY* (rice, TC231874) and *OsCCA1/LHY2* (TC231873). B, *McTOC1* tree. *McTOC1* (GenBank accession no. AY371288), *AtTOC1* (AF272039), *AtAPRR3* (AB046956), *AtAPRR5* (AB046955), *AtAPRR7* (AB046954), *AtAPRR9* (AB046953), *OsTOC1* (rice, TIGR rice pseudomolecules ch. 2 9630.t03778, TC235603) and *TaTOC1* (wheat, TC150832). C, *McELF4* tree. *McELF4* (AY371289), *AtELF4* (At2g40080), *AtELF4-like* (At1g17455), *AtELF4-like* (At1g72630), *AtELF4-like* (At2g29950), *AtELF4-like* (At2g06255), *OsELF4-like* (rice, AF119222, AF161269 ch. 11), *GmELF4-like* (soybean, TIGR TC166607), *LeELF4-like* (tomato, TC118553), and *MtELF4-like* (barrel medic; TC80100). D, *McZTL* and *McFKF1* tree. *McZTL* (AY371290), *McFKF1* (AY371291), *AtZTL* (AF254413), *AtFKF1*

closely related to *AtTOC1/AtAPRR1* (44.5% identity; Fig. 1B). The wheat (*Triticum aestivum*) and rice *TOC1* orthologs (*TaTOC1* and *OsTOC1*) form a separate branch of the tree but are clearly more closely related to *AtTOC1* than *AtAPRR3*, *AtAPRR5*, *AtAPRR7*, and *AtAPRR9*. *McELF4* (AY371289) and *AtELF4* show 41% identity overall and the phylogenetic tree indicates that *McELF4* is most closely related to *AtELF4* and *LeELF4-like* when compared to the 4 Arabidopsis *ELF4*-like genes (Fig. 1C). The rice *ELF4*-like gene falls among *AtELF4*-like genes on a separate branch of the tree to *AtELF4*. We also identified 2 *ELF4*-like sequences from the model legumes barrel medic (*Medicago truncatula*) and soybean (*Glycine max*; *MtELF4*-like and *GmELF4*-like), and these form a third branch on the *ELF4*-tree.

The phylogenetic tree in Figure 1D provides good support for *McZTL* (AY371290; 72% identity with *AtZTL*) and *McFKF1* (AY371291; 80.4% identity with *AtFKF1*) being the closest orthologs of the respective Arabidopsis genes. The rice, wheat, and barley sequences all have highest similarity to *AtFKF1*. A rice gene was identified on chromosome 11 and termed *OsFKF1* because it clusters with *AtFKF1* and *McFKF1* (Fig. 1D). The analysis precluded a precise placement of the other monocot sequences in relation to *ZTL*, *FKF1*, or *LKP2*. The alignment of *McELF3* (AY371292) with *AtELF3* (34.3% identity) was restricted to conserved blocks identified previously in alignments of *AtELF3* with a number of homologous ESTs (Hicks et al., 2001; Liu et al., 2001). In other regions of the protein, *McELF3* shows limited similarity to *AtELF3* or to the *OsELF3* orthologs. *McELF3* is most similar to *AtELF3* rather than to *AtEEC*, which lies on a separate branch of the tree (Fig. 1E). The two rice *OsELF3*-like sequences are highly similar to one another and are orthologs of *AtELF3*.

Temporal Transcript Abundance Profiles of Central Clock Genes in C₃ and CAM *M. crystallinum* Leaves in Light/Dark Cycles and Free-Running Conditions

Transcript abundance profiles for the *M. crystallinum* clock gene orthologs were established in the leaves of both young C₃ and older CAM-induced plants using semiquantitative RT-PCR. We examined the transcript abundance of each gene in both 12-h-light/12-h-dark (LD) cycles and continuous light (LL) to determine whether each gene oscillates in response to either light/dark cycles or a circadian clock. Abundance of *McUBQ10* (TIGR TC4886) was used as a loading control and all data were normalized to the *McUBQ10*

(AF216523), *AtLKP2* (AB038797), *OsFKF1* (rice, TIGR rice pseudomolecules ch. 11 9639.t03046), *OsZTL/FKF1/LKP2* (rice; TIGR pseudomolecules ch. 2 9630.t00468, TC217395), *TaZTL/FKF1/LKP2* (wheat, TC174398), and *HvZTL/FKF1/LKP2* (barley, TC111655). E, *McELF3* tree. *McELF3* (AY371291), *AtELF3* (At2g25930), *AtEEC* (At3g21320), *OsELF3* Ch.1 (rice, AP000399), and *OsELF3* Ch. 6 (rice, AP003296). ch, Chromosome.

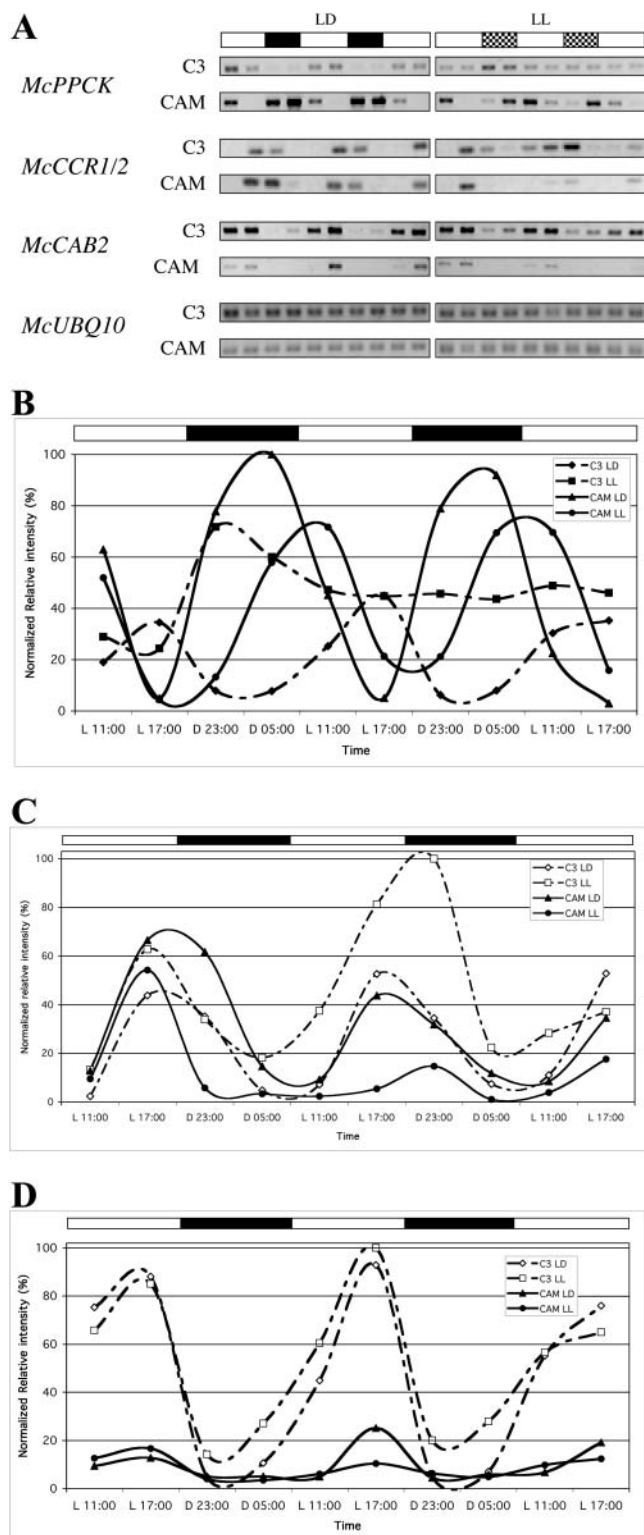


Figure 2. CAM induction mediates alterations in the diurnal and circadian control of *McPPCK* and *McCAB2*. C_3 - and CAM-induced *M. crystallinum* were entrained in LD (12/12) for 29 d (C_3) or 65 d (CAM). CAM-induced plants had been salt stressed for 19 d to ensure complete induction of CAM. At the start of the experiment, one-half of the plants were maintained in LD while one-half were transferred to LL. Leaf samples were collected in duplicate at the indicated time points

signal (Fig. 2A). As controls for CAM induction and evening- and day-expressed clock-controlled genes (CCG), we monitored the transcript abundance of *McPPCK* (AF158091) as a known CAM-induced CCG, a *McCRR1/2* ortholog (TC6352) as a known evening-expressed CCG, and *McCAB2* (AF003128) as a known day-expressed CCG (Fig. 2). While *McPPCK* has previously been reported to be a CCG in CAM-induced leaves, with transcript abundance peaking in the night under the control of the circadian clock, our data show that *McPPCK* transcripts are not under the control of the clock in C_3 *M. crystallinum* (Taybi et al., 2000; Dodd et al., 2003; Fig. 2B). In fact, in C_3 leaves illuminated at a light intensity of 500 to 550 $\mu\text{E m}^{-2} \text{s}^{-1}$, *McPPCK* transcript levels are light-induced and in C_3 , LL *McPPCK* transcripts plateau at a high, light-induced signal with no clear evidence of clock control. These data demonstrate a clear phase shift in the transcript peak of *McPPCK* with the transition of CAM leaves from LD to LL. In LD cycles, *McPPCK* transcript levels peak predawn, while in LL conditions, the transcript levels peak 6 h later in the midmorning. This demonstration of circadian-controlled *McCRR1/2* and *McCAB2* expression in *M. crystallinum* is noteworthy. Furthermore, the peak expression of *McCRR1/2* in the evening (Fig. 2C) and *McCAB2* in the day (Fig. 2D) matches the expression pattern for the corresponding genes in *Arabidopsis*. In LD cycles, the peak level of *McCRR1/2* transcripts in the evening is largely unaffected by CAM induction (Fig. 2C), while the peak level of *McCAB2* transcripts is strongly repressed (approximately 5-fold) by CAM induction (Fig. 2D).

The transcript abundance of *McCCA1/LHY* displays robust oscillations in C_3 and CAM leaves (Fig. 3A). There was little difference between the maximum level of transcript detected in the C_3 and CAM leaf samples. This indicates that the clock control of *McCCA1/LHY* is not affected by CAM induction (Fig. 3A). The peak of *McCCA1/LHY* transcripts occurs after dawn, but expression is also high predawn, indicating a broad dawn-phased peak of transcript (Fig. 3A). This phased expression of *McCCA1/LHY* is in keeping with the circadian control of *CCA1/LHY* in *Arabidopsis* (Wang and Tobin, 1998). In contrast, *McTOC1* transcript levels peak at 5 PM when *McCCA1/LHY* levels decline rapidly (Fig. 3B). One notable feature of C_3 *McTOC1* transcript abundance is that in LL, the peak of *McTOC1* transcripts is phase delayed 6 h to a peak at 11 PM. Furthermore, there is evidence that the steady-state transcript abundance of *McTOC1* increased in the CAM

and RNA was isolated. Semiquantitative RT-PCR was performed on the RNA and the resulting band intensities were normalized to the *McUBQ10* loading control. Diamonds, C_3 in LD; squares, C_3 in LL; triangles, CAM in LD; and circles, CAM in LL. A, Gel images for *McPPCK*, *McCRR1/2*, *McCAB2*, and *McUBQ10*. B, Normalized data for *McPPCK* transcript abundance. C, Normalized data for *McCRR1/2* transcript abundance. D, Normalized data for *McCAB2* transcript abundance.

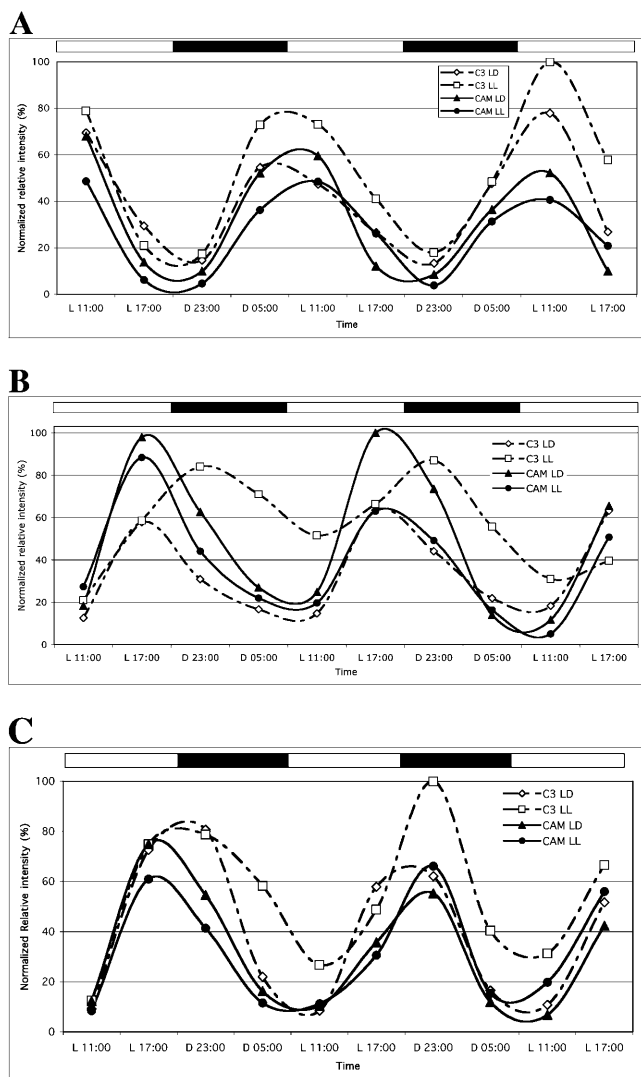


Figure 3. *McCCA1/LHY*, *McTOC1*, and *McELF4* are clock controlled in both C_3 and CAM leaves. *M. crystallinum* plants were entrained in LD (12/12) for 29 d (C_3) or 65 d (CAM). CAM-induced plants had been salt stressed for 19 d to ensure complete induction of CAM. At the start of the experiment, one-half of the plants were maintained in LD while one-half were transferred to LL. Leaf samples were collected at the indicated time points and RNA was isolated. Semiquantitative RT-PCR was performed on the RNA and the resulting band intensities were normalized to the *McUBQ10* loading control. Diamonds, C_3 in LD; squares, C_3 in LL; triangles, CAM in LD; and circles, CAM in LL. A, *McCCA1/LHY* transcript abundance. B, *McTOC1* transcript abundance. C, *McELF4* transcript abundance.

leaves (compare C_3 LD with CAM LD in Fig. 3B). The transcript abundance profiles for *McCCA1/LHY* and *McTOC1* are consistent with reciprocal regulation, as has also been reported for Arabidopsis (Fig. 3, A and B; Alabadi et al., 2001). When *McCCA1/LHY* transcripts are high in the morning, *McTOC1* transcripts reach their trough, and when *McTOC1* transcripts peak in the late afternoon, *McCCA1/LHY* declines rapidly toward an evening trough (Fig. 3, A and B).

The transcript abundance of *McELF4* displays robust oscillations in both C_3 and CAM leaves of *M. crystallinum* under LD and LL (Fig. 3C). *McELF4* transcript levels reach their peak around subjective dusk and their trough around subjective dawn. This abundance profile is compatible with the proposed role of *AtELF4* as part of the evening-expressed mechanism of the central clock (Doyle et al., 2002).

The transcript abundance profiles of the 2 *ZEITLUPE* family genes *McZTL* and *McFKF1* were found to be under circadian control in C_3 and CAM *M. crystallinum* (Fig. 4, A and B). In C_3 leaves, *McZTL* transcript levels peak in the afternoon and reach their trough in the morning. In CAM-induced leaves, *McZTL* transcripts also peak in the afternoon, but *McZTL* transcripts are high between the morning and the evening in CAM leaves, reaching a sharp trough before subjective dawn (Fig. 4A). It is clear that the circadian transcript abundance profile of *McZTL* changes with CAM induction with a more prolonged period of high transcript abundance in the CAM leaves. *McFKF1* transcripts peak sharply in the afternoon and are low to undetectable throughout the remainder of the 24-h cycle (Fig. 4B). In Arabidopsis, *FKF1* transcript levels peak 7 to 10 h after subjective dawn, while *McFKF1* transcripts peak 9 h after subjective dawn (Nelson et al., 2000; Fig. 4B).

McGI transcript levels oscillate in C_3 and CAM leaves with peak transcript levels occurring in the afternoon (Fig. 4C). *McGI* transcripts reach their trough before subjective dawn. Again, this is consistent with the circadian transcript profile of *GI* in Arabidopsis. In Arabidopsis, *AtGI* transcript levels peak in the evening, between 8 and 12 h after dawn, while in *M. crystallinum*, *McGI* transcript levels peak 9 h after dawn (Fowler et al., 1999; Park et al., 1999; Fig. 4C).

The transcript level of *McELF3* is under circadian control in C_3 and CAM leaves (Fig. 4D). Transcripts of this gene increase in the latter part of the day and remain on throughout the night. This is consistent with the *McELF3* gene playing a role in gating the input of light signals to reset the clock in *M. crystallinum*, as has been demonstrated for the Arabidopsis *ELF3* gene (McWatters et al., 2000). In both C_3 and CAM *M. crystallinum* leaves, *McELF3* transcripts reach their trough in the morning after subjective dawn.

Clock Operation during Development and in Response to Salt Stress

For the transcript abundance analysis shown in Figures 2 to 4, we used 29- to 31-d-old plants (measured from the day of seed sowing) as the C_3 plants, and 65- to 67-d-old mature plants that had been salt stressed with 500 mM NaCl for almost 3 weeks as the CAM plants. These plants were chosen to directly compare fully C_3 leaves with fully CAM-induced leaves. This raises the possibility that the changes in the expression of *McTOC1* and *McZTL* that we identified in the experiment in Figures 2 to 4 may be due

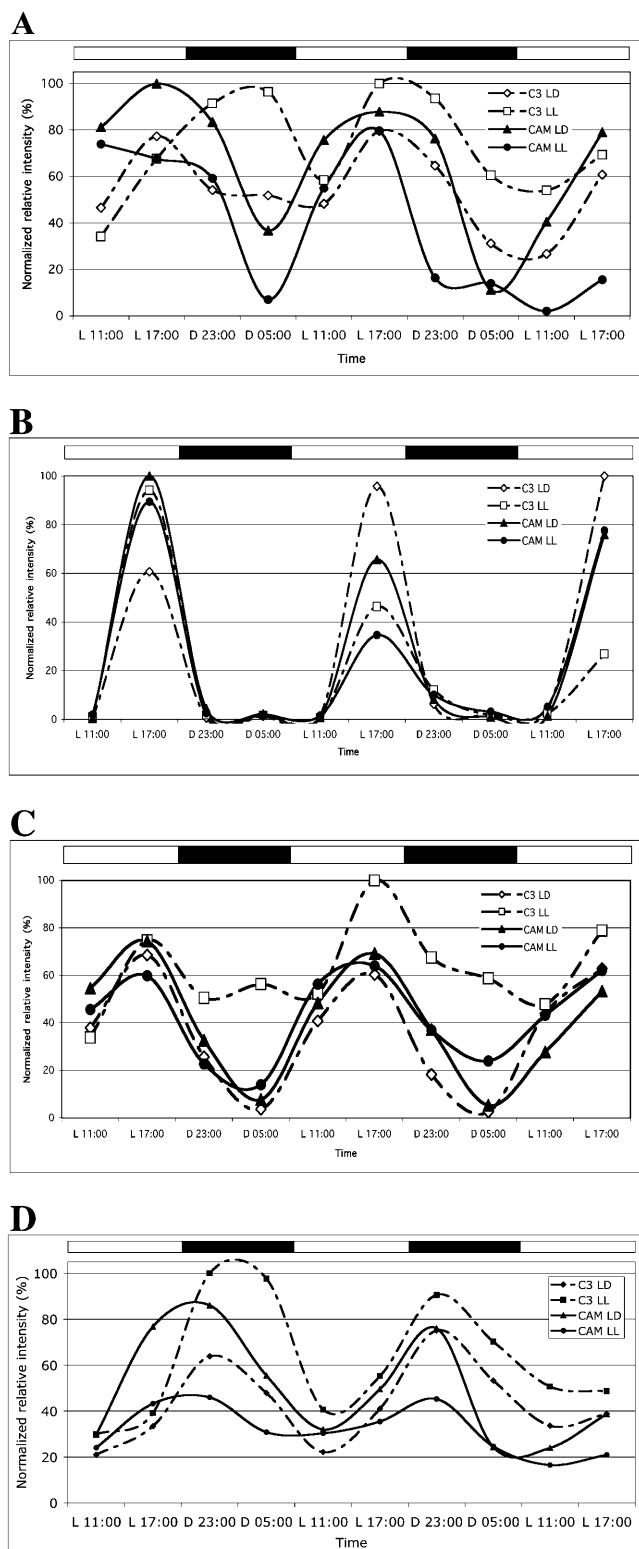


Figure 4. *McZTL* is a clock-controlled gene in C_3 and CAM leaves of *M. crystallinum*. C_3 - and CAM-induced *M. crystallinum* plants were entrained in LD (12/12) for 29 d (C_3) or 65 d (CAM). CAM-induced plants had been salt stressed for 19 d to ensure complete induction of CAM. At the start of the experiment, one-half of the plants were maintained in LD while one-half were transferred to LL. Leaf samples were collected at the indicated time points and RNA was isolated.

to plant development or salt stress or the interaction of both factors. To investigate whether the regulation of the components of the central circadian clock is influenced by development or salt stress, we sampled *M. crystallinum* plants every 2 weeks between 2 and 10 weeks of age. For each age group of plants, one-half were salt stressed with 500 mM NaCl for 1 week prior to sampling, while one-half of the plants were maintained well watered as a control. It should be noted that we grew the plants in 1-L pots and thus we cannot rule out the possibility that the well-watered plants were subjected to mild water stress as their root volume increased over time. We collected leaf samples at 5 AM (3 h prior to dawn) and 5 PM (3 h prior to dusk) and isolated RNA. We then performed semiquantitative RT-PCR to determine the steady-state transcript abundance of each of the clock-associated genes throughout development with and without salt stress. This analysis revealed that the transcript abundance of the majority of the *M. crystallinum* clock-associated genes is remarkably constant throughout development and in response to salt stress (Fig. 5, A–H). Unlike the other clock genes, which all show a good differential in transcript abundance between 5 AM and 5 PM, there is very little difference in the transcript abundance of *McELF3* between 5 AM and 5 PM in Figure 5H, despite the fact that *McELF3* is clearly a CCG (Fig. 4D). Comparison of the 5 AM and 5 PM time points in Figure 4D reveals that *McELF3* transcript levels differ less at these 2 time points in LD cycles. At 5 AM, *McELF3* levels are decreasing to their trough at 11AM, while at 5 PM, *McELF3* levels are increasing to their peak at 11 PM.

CAM genes have previously been reported to be repressed by salt stress in *M. crystallinum* (Kore-eda et al., 2004). The 5 PM peak in the transcript abundance of *McCAB2* is salt repressed in 2-, 4-, and 6-week-old plants (Fig. 5I). There is also a significant developmental decrease in *McCAB2* transcript levels. Even though salt stress causes a repression of *McCAB2* in 2-, 4-, and 6-week-old plants, there is still an additional developmental repression of *McCAB2* as the plants age (Fig. 5I). In 10-week-old plants, peak levels of *McCAB2* are low with and without salt stress (Fig. 5I).

The regulation of the transcript level of *McPPCK* throughout development, with and without salt stress, is very interesting (Fig. 5J). This gene is generally regarded as a salt-induced CAM-specific gene (Taybi et al., 2000; Dodd et al., 2003). However, only in the 2-week-old unstressed plants are *McPPCK* transcript levels low both predawn and predusk. A week of salt stress induces *McPPCK* levels very strongly in the dark at 5 AM even in these 2-week-old plants. We did not see

Semiquantitative RT-PCR was performed on the RNA and the resulting band intensities were normalized to the *McUBQ10* loading control. Diamonds, C_3 in LD; squares, C_3 in LL; triangles, CAM in LD; and circles, CAM in LL. A, *McZTL* transcript abundance. B, *McFKF1* transcript abundance. C, *McGI* transcript abundance. D, *McELF3* transcript abundance.

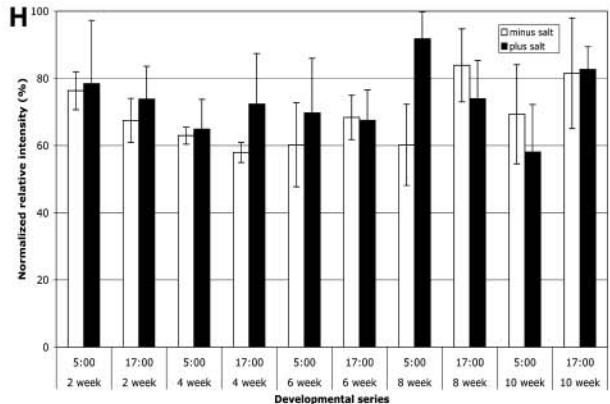
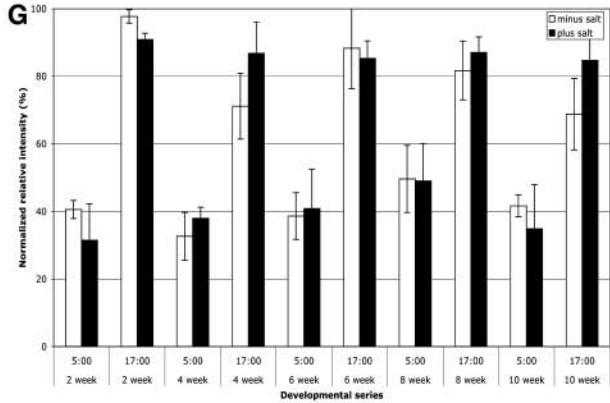
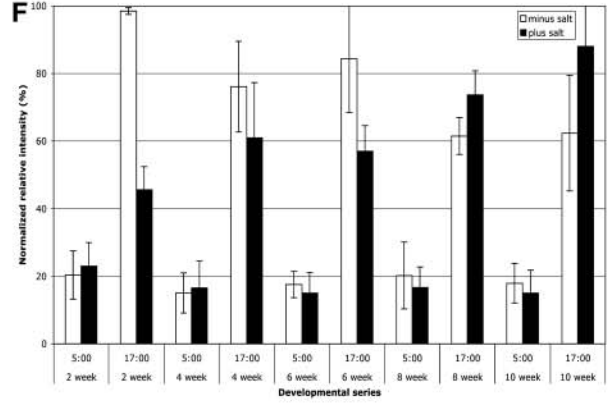
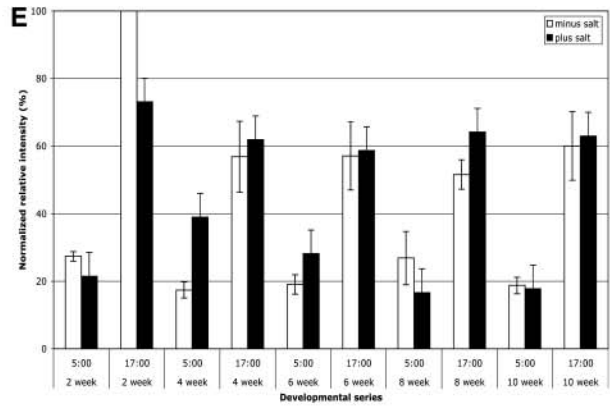
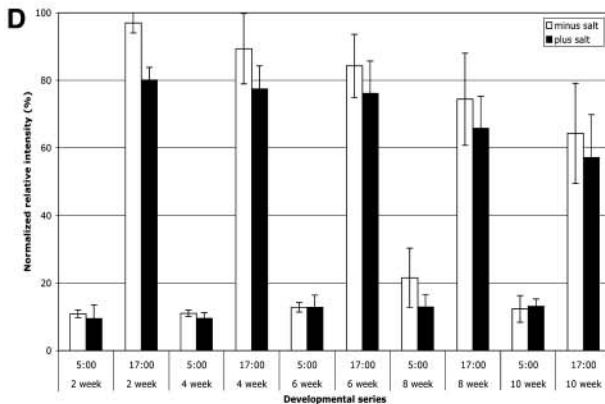
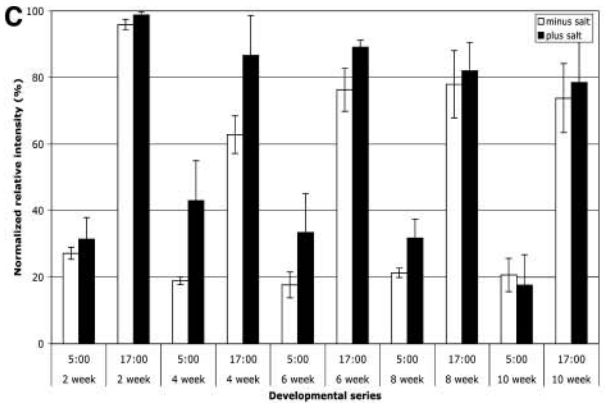
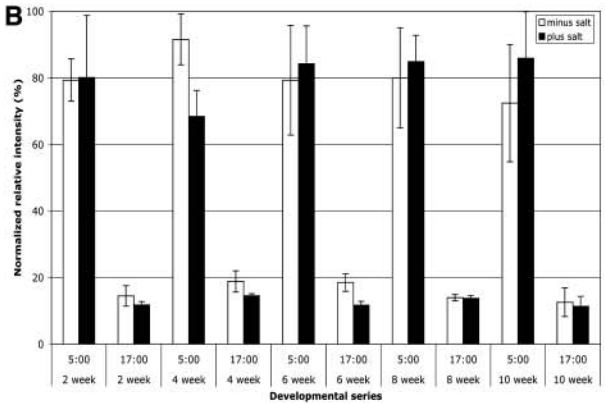
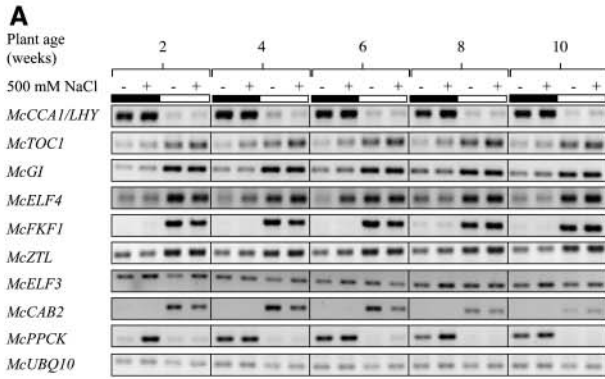


Figure 5. (Legend appears on following page.)

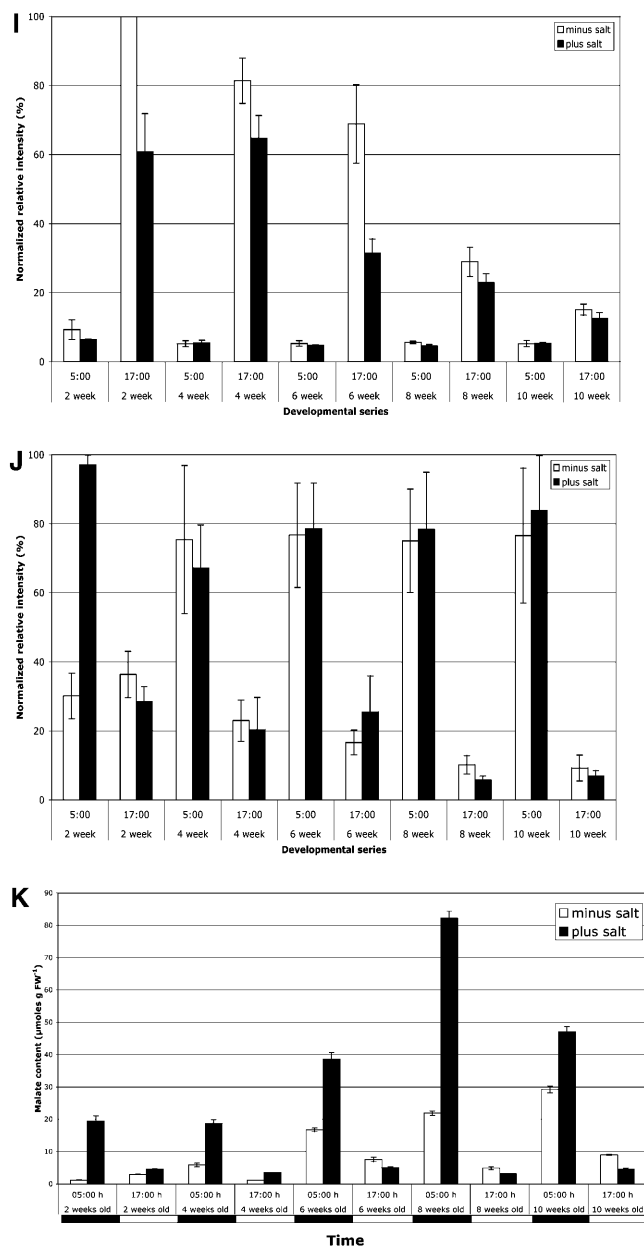


Figure 5. The transcript abundance of clock-associated genes shows compensation against development and salt stress. *M. crystallinum* plants were grown in 12/12 LD cycles. Salt-stressed plants were irrigated with 500 mM NaCl for 1 week prior to sampling. Leaf samples were collected at 5 AM, 3 h prior to dawn, and at 5 PM, 3 h prior to dusk, from plants that were 2, 4, 6, 8, and 10 weeks old, and RNA was isolated. Semiquantitative RT-PCR was performed on the RNA. *McUBQ10* was amplified from the same RNA samples to check the RNA loading. A, Typical gel image for the clock-associated genes plus *McPPCK* and *McCAB2*. B to J, Average normalized relative intensity of triplicate biological replica experiments. The error bars represent the sd. B, *CCA1*. C, *TOC1*. D, *GL1*. E, *ELF4*. F, *FKF1*. G, *ZTL*. H, *ELF3*. I, *CAB2*. J, *PPCK*. K, Leaf malate content was determined for the same leaf samples as an indicator of nocturnal malate accumulation due to the operation of CAM.

light induction of *McPPCK* in the 2-week-old unstressed plants used in this experiment, unlike the light induction observed in the C_3 plants used in the experiment in Figure 2. This is most likely due to the fact that the plants for the experiment shown in Figures 2 to 4 were grown at 500 to 550 $\mu\text{mol photons m}^{-2} \text{s}^{-1}$, while the plants used in the experiment in Figure 5 were grown at 300 to 330 $\mu\text{mol photons m}^{-2} \text{s}^{-1}$. It is well known that the magnitude of the light induction of *PPCK* activity and *PPCK* transcripts in C_3 and C_4 plants is dependent on the light intensity (Nimmo et al., 1987; Bakrim et al., 1992; Fontaine et al., 2002; Marsh et al., 2003). Our data suggest this is also true for *McPPCK* in unstressed leaves of *M. crystallinum* that are performing C_3 photosynthesis. In all the other plants, from 4 to 10 weeks old, *McPPCK* transcripts are present in the dark even in the well-watered control plants. Salt stress has little effect on the *McPPCK* level in these older plants. It is clear that the unstressed nocturnal level of *McPPCK* in the 4- to 10-week-old plants is substantial. This suggests that a key molecular component of the circadian control of CAM is nocturnally expressed in unstressed plants from 4 weeks old onward. Examination of the malate content of the same leaf samples used for RNA isolation revealed that malate levels were higher at 5 AM than at 5 PM, indicative of nocturnal CO_2 fixation via *PEPc* associated with CAM, in all but the 2-week-old unstressed plants in which the malate level is higher at 5 PM and *McPPCK* levels are low at both 5 AM and 5 PM (Fig. 5K). Although *McPPCK* transcripts are high at 5 AM in the 4-week-old unstressed plants, the amount of malate accumulated is low (6 $\mu\text{mol g}^{-1}$ fresh weight) compared to the level in the 4-week-old salt-stressed leaves (19 $\mu\text{mol g}^{-1}$ fresh weight) in which the level of *McPPCK* transcripts at 5 AM is very similar to that in the unstressed leaves. Clearly, the 4-week-old unstressed leaves are performing only a little nocturnal malate accumulation. Examination of the transcript levels for several other CAM-associated genes (e.g. *PEPc*, malic enzyme, and enolase), which are known to be induced by salt stress during the induction of CAM, revealed that these genes were not induced in the 4-week-old unstressed leaves, suggesting that even if the plants had experienced mild water limitation due to their limited 1-L pot size, this was not sufficient to induce CAM (data not shown). Thus, the nocturnal induction of *McPPCK* in 4-week-old unstressed plants is not indicative of the leaves performing significant CAM as judged by malate accumulation. Examination of the regulation of *McPPCK* transcript levels throughout the dark period in 4-week-old unstressed leaves and 8-week-old stressed leaves revealed that, while *McPPCK* transcripts are high in the 4-week-old unstressed leaves at the 5 AM time point reported here and at 8 AM, they are low earlier in the night at 8 PM, 11 PM, and 2 AM (data not shown). However, the 8-week-old salt-stressed leaves have high *McPPCK* transcript levels at 11 PM, 2 AM, 5 AM, and 8 AM, revealing a significantly prolonged peak of *McPPCK* transcript

abundance in these older stressed leaves (data not shown). Thus, the substantially greater malate accumulation at 5 AM in the 8-week-old stressed leaves correlates with a much broader or more prolonged peak of *McPPCK* levels. This important result indicates that it is not the quantity of *McPPCK* at a particular time point during the night that is important for determining the capacity for nocturnal malate accumulation, but the duration of the *McPPCK* transcript peak throughout the night.

DISCUSSION

Circadian Clock Genes in *M. crystallinum*

We have cloned the *M. crystallinum* orthologs corresponding to seven plant circadian clock-associated genes. All seven of the *M. crystallinum* genes reported here were cloned and characterized from the model C_3 plant Arabidopsis. This report of the cloning and characterization of all clock-associated genes in a second plant species not only documents evolutionary conservation and adaptation of the clock function, but also provides information about clock functioning in a CAM plant and compensation of the clock against development and abiotic stress.

Our phylogenetic analysis of the available full-length *CCA1/LHY* sequences reveals some very interesting points. First, Arabidopsis is the only species that possesses 2 genes belonging to the *CCA1/LHY* family. The two rice sequences in our phylogenetic tree represent transcripts from a single gene. A BLAST search against the TIGR rice genome database (http://tigrblast.tigr.org/euk-blast/index.cgi?project=osa1&database=Genes_in_TIGR_Rice_Pseudomolecules) revealed only 1 rice *OsCCA1/LHY*-related sequence on chromosome 8, and this is the gene that encodes *OsCCA1/LHY* and *OsCCA1/LHY2*. Furthermore, the TIGR TC sequences from which we derived the 2 rice genes in Figure 1A align perfectly, except for a small number of base changes (23 out of 3,499 bases for *OsCCA1/LHY* compared to *OsCCA1/LHY2*) and 5 gaps (30–160 bp in length), suggesting that *OsCCA1/LHY* and *OsCCA1/LHY2* are splice variants from the same gene. *OsCCA1/LHY* contains 4 unspliced introns that are not present in *OsCCA1/LHY2*. However, it is noteworthy that the unspliced introns do not create premature stop codons and thus the unspliced version of the *OsCCA1/LHY* transcript could encode a functional protein. The rice *OsCCA1/LHY* gene clearly merits further investigation in relation to alternative splicing. Second, all of the available monocot *CCA1/LHY* sequences are most closely related to *AtCCA1*, revealing that *AtCCA1* itself has evolved relatively slowly since the monocot-dicot split. To improve our understanding of the evolution of the plant circadian clock, it will be important to determine whether other dicot species possess 2 genes in the *CCA1/LHY* family as the Arabidopsis paradigm might suggest.

The *TOC1* phylogenetic tree shows that *McTOC1* is the nearest neighbor to *AtTOC1* (Fig. 1B). There are numerous plant ESTs that encode fragments of *TOC1* genes from other species, but only ESTs from rice and wheat assemble into full-length *TOC1* sequences (Fig. 1B). As in *AtTOC1*, in *McTOC1* the 2 Asp residues that are essential for phosphorelay in response regulator proteins are changed to Glu (Asp-1) and Asn (Asp-2; Strayer et al., 2000). This implies that these residues may themselves play an important role in the function of the pseudoregulator domain of *TOC1* because they are conserved between the Aizoaceae and the Brassicaceae. The C-terminal CONSTANS domain of *AtTOC1* is also well conserved in *McTOC1*, and C terminal to this motif is a region rich in acidic residues. Overall, the C termini of the 2 proteins (from residue 512 of *AtTOC1* and 444 of *McTOC1* to the C terminus) are 61% identical. The C-terminal acidic region is less highly conserved in the other Arabidopsis pseudoregulator proteins *APRR3*, *APRR5*, *APRR7*, and *APRR9*. For example, the C terminus of *McTOC1* (from residue 444 to the C terminus) shares between 33% and 42% identity with the C terminus of *AtAPRR3*, *AtAPRR5*, *AtAPRR7*, and *AtAPRR9*. Such an acidic region is a common feature of many transcriptional activators, and the conservation of this region among the *TOC1* genes implies they may act as transcription factors.

McELF4 is clearly a good ortholog of *AtELF4* (Fig. 1C). The *ELF4* genes encode very small, nuclear localized proteins of around 110 amino acid residues with no known functional domains (Doyle et al., 2002; Khanna et al., 2003). Only 22 residues are identical between all of the available *ELF4* and *ELF4-like* sequences.

McZTL and *McFKF1* were named based on their phylogenetic relationships revealed in the tree in Figure 1D. The gene duplication event that generated these two genes clearly predates the separation of the Aizoaceae and the Brassicaceae from their common ancestor. *AtLKP2* sits alone on a separate branch of the tree, suggesting that there could be a *McLKP2* gene in the *M. crystallinum* genome. The *ZEITLUPE* family of proteins in Arabidopsis contains 3 conserved protein motifs: a LOV-type PER ARNT SIM domain near the N terminus, a 40-amino acid F-box in the center of the protein, and 6 C-terminal kelch repeats. All 3 of these motifs are conserved in *McZTL* and *McFKF1*, indicating that the proteins are likely to function in a similar manner in *M. crystallinum*.

McELF3 is most closely related to *AtELF3*. *ELF3* is a novel protein that lacks identifiable protein motifs. However, *ELF3* does align with short ESTs from a range of plant species, and this has allowed a number of *ELF3* conserved domains to be identified (Hicks et al., 2001; Liu et al., 2001). All of these domains are conserved in *McELF3*. *AtELF3* is nuclear localized, but the putative nuclear localization signal is poorly conserved in *McELF3* (2 out of 7 residues identical; Hicks et al., 2001). Furthermore, only a single residue of the putative *AtELF3* nuclear localization signal is

conserved in the rice *ELF3* orthologs. However, *McELF3* is predicted to be nuclear localized based on its generally basic sequence (PSORTII; Reinhardt's method gives a 94.1% reliability that *McELF3* is nuclear localized; k-NN prediction gives a 65.2% probability that *McELF3* localizes to the nucleus).

McPPCK and *McCCR1/2* Regulation in *M. crystallinum*

McPPCK transcript levels show a 6-h phase delay in their peak in LL conditions in CAM leaves (Fig. 2B). This phase delay in LL has not been reported previously and is important in terms of understanding CAM CO₂ fixation rhythms in LL. None of the central clock genes that we have studied display a similar phase delay in CAM leaves in LL. This suggests that if the *CCA1/LHY* and *TOC1* oscillator is providing the temporal information that coordinates *McPPCK* during CAM, then the output pathway that links the central clock to *McPPCK* must include an element that undergoes a phase delay relative to the underlying oscillator when CAM leaves are transferred to LL. Alternatively, *McPPCK* control may occur via a different oscillator that is phase delayed in LL.

Our analysis of the regulation of *McCCR1/2* cycling in LL (Fig. 2, A and C) reveals that, while this gene oscillates robustly in C₃ leaves, the oscillations damp out very rapidly in CAM-induced leaves. However, *McCCR1/2* transcript levels do cycle in CAM leaves under driven LD conditions, so it is clear that *McCCR1/2* may be specifically uncoupled from its clock in CAM-induced leaves. In *Arabidopsis*, *AtCCR2* expression is controlled in part by its own protein in a suboscillator feedback loop (Heintzen et al., 1997). This makes it possible that the autoregulation of *McCCR1/2* is lost in salt-stressed, CAM-induced leaves even though the central clock itself is largely compensated against stress and continues to operate robustly in CAM-induced leaves.

The *M. crystallinum* Clock Genes Are Themselves Clock Controlled

Our analysis of the regulation of the clock-associated genes in C₃ and CAM leaves allowed us to discern two key points about the control of the transcript level of these genes in *M. crystallinum*. First, the transcript abundance of all seven clock-associated genes not only oscillated in LD, but also continued to oscillate in LL. Second, we identified *McZTL* as the one gene whose transcript abundance profile differs from its *Arabidopsis* ortholog. *AtZTL* transcripts do not oscillate in LD or LL (Somers et al., 2000), but we have demonstrated that *McZTL* transcripts oscillate in LD and LL in both C₃ and CAM leaves.

The amplitude of the oscillations in the relative transcript abundance of *McCCA1/LHY* changes little with CAM induction. This supports the hypothesis that these single Myb-repeat transcription factors form part of the central oscillator in *M. crystallinum*. If the

transcript abundance of these genes changed markedly with the C₃-to-CAM switch, it would suggest that the clock includes other components that are more important for maintaining robust rhythmicity throughout the life of the plant. It is of particular interest in this context to note that the relative transcript abundance for three isoforms of the light-harvesting chlorophyll *a/b*-binding protein (*McCAB*) oscillated in both C₃ and CAM *M. crystallinum* (Fig. 2D; data not shown). Although rhythmicity of the *McCAB* transcript oscillations is maintained between C₃ and CAM, the amplitude of *McCAB* rhythms decreases significantly between C₃ leaves and CAM leaves because *McCAB* genes are repressed by CAM induction (Fig. 2D). The *AtCCA1/LHY* transcription factors bind to the promoter of *AtCAB* genes and mediate both the acute response of these genes to light and their circadian regulation (Wang et al., 1997; Wang and Tobin, 1998). It is therefore significant that, although *McCAB* gene transcript levels are repressed after CAM induction, *McCCA1/LHY* levels are relatively unchanged between C₃ and CAM. This suggests the existence of a repressor protein binding to the *McCAB* promoters to down-regulate their expression in CAM-induced leaves. Alternatively, these transcripts are globally repressed as a result of stress treatment and/or are selectively targeted for turnover following stress.

Our data on the transcript profile of *McZTL* in C₃ and CAM *M. crystallinum* demonstrate that, during plant evolution, the control of the *ZTL* gene has altered between a member of the Aizoaceae and a member of the Brassicaceae. Conservative estimates, based on the fossil record, of the dates of divergence of the major eudicot clades put the date of divergence of the Brassicales (*Arabidopsis*) at 89.5 million years ago and the Caryophyllales (*Mesembryanthemum*) at 83 million years ago (<http://www.flmnh.ufl.edu/deeptime>). Thus, a change has occurred in the regulation of the transcript abundance of *ZTL* between *Arabidopsis* and *Mesembryanthemum* sometime in the last 80 to 90 million years. Recently, *AtZTL* has been reported to be regulated posttranscriptionally via different circadian phase-specific degradation rates (Kim et al., 2003). It will be interesting to see whether *McZTL* is also regulated posttranscriptionally via proteasome-dependent proteolytic degradation in *M. crystallinum*, in addition to the circadian control of its relative transcript abundance reported here. Our findings suggest that there will be many subtle differences in the machinery of the plant circadian clock that become apparent as more plant species are studied with respect to their clock genes and the regulatory interactions that constitute the central plant clock. Studying the evolution of the plant clock will undoubtedly provide substantial insight into which genes are the most fundamental components of the central plant clock and which genes are more peripheral and therefore have been subjected to greater or lesser selection pressure during evolution.

The Plant Circadian Clock Is Largely Compensated against Development and Abiotic Stress

Our data examining the influence of development and salt stress on the operation of the central clock (Fig. 5) provide insight into environmental compensation within the plant circadian oscillator. While it is well established that the clock is temperature compensated to permit robust rhythmicity over a broad temperature range (Somers et al., 1998), compensation of the plant clock against other environmental signals has not been examined previously. Our data reveal that the plant clock is largely compensated against severe abiotic stress in the form of 500 mM NaCl. Furthermore, the circadian control of the plant clock genes also changes little during the life of the plant in the absence of salt stress. The fact that the central clock genes operate robustly, showing only relatively small changes throughout the life cycle of *M. crystallinum* even in the face of severe salt stress, is further evidence of just how important the clock is to the competitive success of a plant. By maintaining consistent clock function in a diverse range of conditions, the plant can ensure that it still optimizes the temporal aspects of its metabolism that are vital to reproductive success. This latter point is particularly relevant in a stress-inducible CAM plant, where it is clear that coordination of the CAM pathway by the circadian clock avoids potentially catastrophic futile cycles between malate synthesis and decarboxylation.

The identification of the clock genes reported here in a model inducible CAM plant that can switch rapidly from C₃ to CAM sets the stage for future work aimed at a detailed understanding of the molecular basis of the circadian control of the CAM pathway. We now have the necessary molecular tools to manipulate the expression of these genes in transgenic CAM plants and examine the effect these perturbations have on the circadian control of CO₂ fixation via the CAM pathway. These experiments will allow us to finally resolve the nature of the circadian oscillator that controls CAM.

MATERIALS AND METHODS

Plant Material

Mesembryanthemum crystallinum plants were grown from seed in vermiculite irrigated with half-strength Hoagland solution in a growth chamber on a 12-h-light (23°C)/12-h-dark (18°C) cycle. The photoperiod was for 12 h from 8 AM until 8 PM. Fluorescent lighting provided a photon flux density of 500 to 550 μmol photons m⁻² s⁻¹. Young plants aged 29 d were used for the collection of C₃ leaves and plants that were 65 d old and had been stressed with 500 mM NaCl for 19 d were used for the CAM leaves. One-half of the plants were in LD cycles and one-half were transferred to LL and constant temperature (23°C) at the beginning of the experiment (8 AM, lights on). Duplicate leaf samples were collected every 6 h for a total of 60 h at the following times: 11 AM, 5 PM, 11 PM, and 5 AM, giving a total of 10 time points for each treatment (C₃ LD, C₃ LL, CAM LD, and CAM LL). For the experiment to examine the role of development and salt stress in clock gene control (Fig. 5), the plants were grown in 1-L pots at 300 to 330 μmol photons m⁻² s⁻¹, and the salt-stressed plants were irrigated with 500 mM NaCl for 1 week prior to sampling. All samples were frozen in liquid nitrogen and stored at -80°C until use.

RNA Isolation

Frozen leaf samples were ground in liquid nitrogen using a mortar and pestle, and total RNA was isolated from the frozen powder using a cetyltrimethylammonium bromide-based RNA extraction procedure (Hartwell et al., 1996). Total RNA samples were treated with DNase (DNA-free kit; Ambion., Austin, TX) to eliminate contaminating genomic DNA. Many of the primers used for the amplification of specific genes flanked introns, and contamination by genomic DNA was never detected in any of the RT-PCR reactions. Following DNase treatment, the quantity and purity of the total RNA were determined spectrophotometrically as described (Sambrook et al., 1989). All RNA samples were diluted to a concentration of 0.2 μg/μL prior to use in RT reactions.

Semiquantitative RT-PCR

The total RNA samples (2 μg) were mixed with 1 μg of anchored oligo(dT) (5'-AAGCTTTTTTTTTTTTTT-3') and incubated at 95°C for 2 min and immediately cooled on ice. RT was carried out in a reaction mixture (40 μL) containing the denatured RNA plus oligo(dT), 1× Stratascript RT buffer (Stratagene, La Jolla, CA), 1 mM dNTPs (Invitrogen, Carlsbad, CA), and 40 units of Stratascript RT (Stratagene). The reaction was incubated at 37°C for 90 min, followed by 95°C for 5 min.

PCR reactions were performed using 1 μL of each reverse transcribed cDNA sample in a reaction mixture (10 μL) containing 1× Sigma ReadyMix REDTaq PCR reaction mix with MgCl₂ (Sigma, St. Louis) and 1 μM of each forward and reverse primer. The primer sequences and the predicted product sizes are indicated in Table I. PCR reactions were conducted in a programmable thermocycler (PTC200 DNA engine; MJ Research, Watertown, MA), and the optimal number of PCR cycles for each gene is indicated in Table I. Standard PCR cycles were 95°C for 2 min, a gene-specific number of cycles of 55°C/30 s, 72°C/1 min, 95°C/30 s, and a final extension step of 55°C for 30 s followed by 72°C for 7 min. All products were separated on a 1% agarose gel in 1× Tris-acetate EDTA and stained with ethidium bromide. Gels were visualized using a Bio-Rad gel documentation system and band intensities were quantified using Quantity One software (Bio-Rad Laboratories, Hercules, CA). An *M. crystallinum* polyubiquitin gene (*McUBQ10*; TIGR TC4886) with high homology to Arabidopsis (*Arabidopsis thaliana*) *UBQ10* was used as the loading control for the RT-PCR. The *McUBQ10* primer sequences used are given in Table I. The quantified RT-PCR signals for all the clock genes examined here were normalized to the *McUBQ10* signal to correct for minor variations in the loading of RNA into the RT reactions and/or the efficiency of the RT reactions. All experiments were carried out in duplicate; in each case, similar trends were observed. The data presented in Figures 2 to 4 are from individual experiments that are representative of the results obtained. The data in Figure 5, B–J, show the mean normalized relative intensity from three biological replicates and the error bars represent the sd. The gel in Figure 5A shows the raw data for a single replicate.

The gene-specific primers for *McCCA1/LHY*, *McELF4*, *McGI*, and *McELF3* were designed to target partial 3' EST sequences corresponding to fragments of the *M. crystallinum* orthologs. The ESTs were identified from the *M. crystallinum* gene index (<http://www.tigr.org/tdb/tgi/mcgi>; Kore-eda et al., 2004) using the TBLASTN search algorithm and the Arabidopsis *CCA1/LHY*, *ELF4*, *GI*, and *ELF3* protein sequences as input sequences. The *FKF1* ESTs have GenBank accession numbers AI026317, AA791399, AA791403, and AI822178. The *CCA1/LHY* ESTs have accession numbers BF479609, BM300086, and BM034918. The *ELF3* EST has accession number BF479720, the *ELF4* EST has accession number CA838873, and the *GI* EST has accession number CA838115.

Degenerate PCR to Clone the *M. crystallinum* ZTL and FKF1 Orthologs

To isolate the *M. crystallinum* cDNA sequences corresponding to the Arabidopsis clock-associated genes *ZTL* and *FKF1*, a degenerate PCR strategy was employed. The degenerate PCR primers ZTLF 5' CAWGGNGADYTDYTNAAAYTTY 3' (corresponding to the conserved amino acid motif QGELLNF), and ZTLR1 5' RCTHGCVYTRDGDARYTCATG 3' and ZTLR2 5' RCTYGCYAARCAHARYTCATG 3' (corresponding to the conserved amino acid motifs HELSLAS found in *AtZTL* and HELCLAS found in *AtFKF1*, respectively) were used. The conserved regions of the *ZEITLUPE* family of

proteins were identified by aligning EST sequences from Arabidopsis, tomato (*Lycopersicon esculentum*), *Sorghum bicolor*, soybean (*Glycine max*), wheat (*Triticum aestivum*), barley (*Hordeum vulgare*), rice (*Oryza sativa*), *Lotus japonicus*, *Zea mays*, *M. crystallinum*, and barrel medic (*Medicago truncatula*).

Cloning a 5' Fragment of the *M. crystallinum* TOC1 Gene

We identified two ESTs from sugar beet (*Beta vulgaris*; accession nos. BI543444 and BI543434) in the GenBank EST database with homology to the 5' end of the Arabidopsis TOC1 gene. Sugar beet, like *M. crystallinum*, is a member of the taxonomic order Caryophyllales, which justified primer design to conserved regions between the sugar beet and Arabidopsis TOC1 orthologs. The primers BvTOC1F 5'-TTCATTGATCGAAGTAAAGTCAG-3' and BvTOC1R 5'-CCAGCCTCAAGCACCATTAC-3' were used to amplify a 311-bp fragment of the *M. crystallinum* TOC1 cDNA via RT-PCR.

Cloning and Sequencing of RT-PCR and RACE-PCR Products

All RT-PCR and RACE-PCR products were gel purified using the QIAquick gel extraction kit (Qiagen, Valencia, CA) and cloned into the TA vector (pCR4-TOPO) using the TOPO TA cloning kit for sequencing (Invitrogen) according to the manufacturer's protocols. The CCA1/LHY 5' RACE-PCR product was sequenced directly by primer walking. Cloned inserts in pCR4-TOPO were sequenced fully on both strands by the in-house DNA-sequencing units at the University of Arizona, Tucson, and the University of Nevada, Reno, to confirm the gene specificity of the RT-PCR reactions. All PCR reactions were found to have targeted the gene of interest.

Cloning the Full-Length cDNAs for CCA1/LHY, TOC1, ELF4, ZTL, FKF1, and ELF3 Orthologs from *M. crystallinum* Using RACE-PCR

The 5' and 3' ends of the *M. crystallinum* CCA1/LHY, TOC1, ZTL, FKF1, ELF4, and ELF3 cDNAs were amplified using the SMART RACE-PCR kit (CLONTECH, Palo Alto, CA) according to the manufacturer's protocols. SMART cDNA was synthesized from total RNA corresponding to the time of the transcript peak for each clock gene as determined with semiquantitative RT-PCR analysis. The gene-specific primer for cloning the 5' end of CCA1/LHY was 5'-CTTGCTGTGGCCAAGGTTTCCTAGC-3'; for the 5' end of ZTL, 5'-AGGAGCAACACCTCCAGGGTTCCAG-3'; for the 3' end of ZTL, 5'-CAAGCACAGTTCATGCACGCTCGATG-3'; for the 5' end of FKF1, 5'-GCAAACCTTAGGTGGCTGACCGGGAAC-3'; for the 5' end of ELF3, 5'-CTGCCGTCTTCTGCTGTATTGACTGG-3'; for the 5' end of TOC1, 5'-TCCTCGGCATTAAGTGCATCAATAACCTG-3'; for the 3' end of TOC1, 5'-TGTGATAACGATTCCAAGAGCTCGAGGAG-3'; for the 5' end of ELF4, 5'-CCCTTCATATTCAATCCACCATTTCTCC-3'; for the 3' end of ELF4, 5'-TGAAGAATGTGGCGATCATTAGGAATG-3'. The 3' end of CCA1/LHY, FKF1, and ELF3 was obtained by sequencing the 3' end of ESTs in the database.

Malate Determination

Samples (500 mg) of the same leaves that were used for RNA isolation (including the duplicate samples) were ground in liquid nitrogen and extracted in 7 mL of 80% methanol at 70°C. The methanol extracts were dried down and resuspended in 0.5 mL 200 mM Bicine, pH 7.8. The concentration of malate was determined using the enzymatic method described by Möllering (1974). Each extract was assayed in triplicate.

DNA and Protein Sequence Analysis

DNA sequence data were analyzed using Vector NTI Suite for MacOSX (Informax, Frederick, MD). Database searches were conducted using the National Center for Biotechnology Information (NCBI) network version of BLAST 2.0 (Altschul et al., 1997). Multiple sequence alignments and phylogenetic trees were generated using the AlignX program within the Vector NTI Suite for MacOSX. AlignX uses a modified ClustalW algorithm to align the

amino acid sequences and builds phylogenetic trees using the neighbor-joining method (Saitou and Nei, 1987).

Upon request, all novel materials described in this publication will be made available in a timely manner for noncommercial research purposes, subject to requisite permission from any third-party owners of all parts of the material. Obtaining any permissions will be the responsibility of the requester.

Sequence data from this article have been deposited in the GenBank/EMBL data libraries under the following accession numbers: McCCA1/LHY, AY371287; McTOC1, AY371288; McELF4, AY371289; McZTL, AY371290; McFKF1, AY371291; and McELF3, AY371292.

ACKNOWLEDGMENTS

J.H. thanks Susie Boxall for working on this project voluntarily. We thank Christine B. Michalowski for growing some of the plants used in this study.

Received October 8, 2004; returned for revision December 23, 2004; accepted January 6, 2005.

LITERATURE CITED

- Alabadi D, Oyama T, Yanovsky MJ, Harmon FG, Mas P, Kay SA (2001) Reciprocal regulation between TOC1 and LHY/CCA1 within the *Arabidopsis* circadian clock. *Science* **293**: 880–883
- Altschul SE, Madden TL, Schäffer AA, Zhang J, Zhang Z, Miller W, Lipman DJ (1997) Gapped BLAST and PSI-BLAST: a new generation of protein database search programs. *Nucleic Acids Res* **25**: 3389–3402
- Bakrim N, Echevarria C, Cretin C, Cretin C, Arriodupont M, Pierre JN, Vidal J, Chollet R, Gadal P (1992) Regulatory phosphorylation of *Sorghum* leaf phosphoenolpyruvate carboxylase. Identification of the protein-serine kinase and some elements of the signal-transduction cascade. *Eur J Biochem* **204**: 821–830
- Borland AM, Hartwell J, Jenkins GI, Wilkins MB, Nimmo HG (1999) Metabolite control overrides circadian regulation of phosphoenolpyruvate carboxylase kinase and CO₂ fixation in Crassulacean acid metabolism. *Plant Physiol* **121**: 889–896
- Carter PJ, Nimmo HG, Fewson CA, Wilkins MB (1991) Circadian rhythms in the activity of a plant protein kinase. *EMBO J* **10**: 2063–2068
- Daniel X, Sugano S, Tobin EM (2004) CK2 phosphorylation of CCA1 is necessary for its circadian oscillator function in *Arabidopsis*. *Proc Natl Acad Sci USA* **101**: 3292–3297
- Dodd AN, Griffiths H, Taybi T, Cushman JC, Borland AM (2003) Integrating diel starch metabolism with the circadian and environmental regulation of Crassulacean acid metabolism in *Mesembryanthemum crystallinum*. *Planta* **216**: 789–797
- Doyle MR, Davis SJ, Bastow RM, McWatters HG, Kozma-Bognár L, Nagy E, Millar AJ, Amasino RM (2002) The *ELF4* gene controls circadian rhythms and flowering time in *Arabidopsis thaliana*. *Nature* **419**: 74–77
- Erikssoon ME, Millar AJ (2003) The circadian clock. A plant's best friend in a spinning world. *Plant Physiol* **132**: 732–738
- Fontaine V, Hartwell J, Jenkins GI, Nimmo HG (2002) *Arabidopsis thaliana* contains two phosphoenolpyruvate carboxylase kinase genes with different expression patterns. *Plant Cell Environ* **25**: 115–122
- Fowler S, Lee K, Onouchi H, Samach A, Richardson K, Coupland G, Putterill J (1999) *GIGANTEA*: a circadian clock-controlled gene that regulates photoperiodic flowering in *Arabidopsis* and encodes a protein with several possible membrane-spanning domains. *EMBO J* **18**: 4679–4688
- Han L, Mason M, Risseuw EP, Crosby WL, Somers DE (2004) Formation of an SCF^{ZTL} complex is required for proper regulation of circadian timing. *Plant J* **40**: 291–301
- Hartwell J, Gill A, Nimmo GA, Wilkins MB, Jenkins GI, Nimmo HG (1999) Phosphoenolpyruvate carboxylase kinase is a novel protein kinase regulated at the level of expression. *Plant J* **20**: 333–342
- Hartwell J, Nimmo GA, Wilkins MB, Jenkins GI, Nimmo HG (2002) Probing the circadian control of phosphoenolpyruvate carboxylase kinase expression in *Kalanchoë fedtschenkoi*. *Funct Plant Biol* **29**: 663–668
- Hartwell J, Smith LH, Wilkins MB, Jenkins GI, Nimmo HG (1996) Higher plant phosphoenolpyruvate carboxylase kinase is regulated at the level

- of translatable mRNA in response to light or a circadian rhythm. *Plant J* **10**: 1071–1078
- Heintzen C, Nater M, Apel K, Staiger D** (1997) AtGRP7, a nuclear RNA-binding protein as a component of a circadian-regulated negative feedback loop in *Arabidopsis thaliana*. *Proc Natl Acad Sci USA* **94**: 8515–8520
- Hicks KA, Albertson TM, Wagner DR** (2001) *EARLY FLOWERING3* encodes a novel protein that regulates circadian clock function and flowering in *Arabidopsis*. *Plant Cell* **13**: 1281–1292
- Imaizumi T, Tran HG, Swartz TE, Briggs WR, Kay SA** (2003) FKF1 is essential for photoperiodic-specific light signalling in *Arabidopsis*. *Nature* **426**: 302–306
- Izawa T, Takahashi Y, Yano M** (2003) Comparative biology comes into bloom: genomic and genetic comparison of flowering pathways in rice and *Arabidopsis*. *Curr Opin Plant Biol* **6**: 113–120
- Kaldis A-D, Kousidis P, Kesanopoulos K, Prombona A** (2003) Light and circadian regulation in the expression of LHY and Lhcb genes in *Phaseolus vulgaris*. *Plant Mol Biol* **52**: 981–997
- Khanna R, Kikis EA, Quail PH** (2003) *EARLY FLOWERING 4* functions in phytochrome B-regulated seedling de-etiolation. *Plant Physiol* **133**: 1530–1538
- Kim W-Y, Geng R, Somers DE** (2003) Circadian phase-specific degradation of the F-box protein ZTL is mediated by the proteasome. *Proc Natl Acad Sci USA* **100**: 4933–4938
- Kore-eda S, Cushman MA, Akseilrod I, Bufford D, Fredrickson M, Clark E, Cushman JC** (2004) Transcript profiling of salinity stress responses by large-scale expressed sequence tag analysis in *Mesembryanthemum crystallinum*. *Gene* **341**: 83–92
- Liu XL, Covington ME, Fankhauser C, Chory J, Wagner DR** (2001) ELF3 encodes a circadian clock-regulated nuclear protein that functions in an *Arabidopsis* PHYB signal transduction pathway. *Plant Cell* **13**: 1293–1304
- Lüttge U** (2000) Tonoplast functioning as the master switch for circadian regulation of Crassulacean acid metabolism. *Planta* **211**: 761–769
- Lüttge U** (2003) Circadian rhythmicity: Is the “biological clock” hardware or software? *Prog Bot* **64**: 277–319
- Marsh JT, Sullivan S, Hartwell J, Nimmo HG** (2003) Structure and expression of phosphoenolpyruvate carboxylase kinase genes in Solanaceae. A novel gene exhibits alternative splicing. *Plant Physiol* **133**: 2021–2028
- Mas P, Kim W-Y, Somers DE, Kay SA** (2003) Targeted degradation of TOC1 by ZTL modulates circadian function in *Arabidopsis thaliana*. *Nature* **426**: 567–570
- McClung CR** (2001) Circadian rhythms in plants. *Annu Rev Plant Physiol Plant Mol Biol* **52**: 139–162
- McWatters HG, Bastow RM, Hall A, Millar AJ** (2000) The *ELF3* *zeitnehmer* regulates light signalling to the circadian clock. *Nature* **408**: 716–720
- Möllering H** (1974) L-malate: determination with malate dehydrogenase and glutamate-oxaloacetate transaminase. In HU Bergmeyer, ed, *Methods of Enzymatic Analysis*, Vol 3. Verlag Chemie, Weinheim, Germany, pp 1589–1593
- Nelson DC, Lasswell J, Rogg LE, Cohen MA, Bartel B** (2000) *FKF1*, a clock-controlled gene that regulates the transition to flowering in *Arabidopsis*. *Cell* **101**: 331–340
- Nimmo GA, McNaughton GAL, Fewson CA, Wilkins MB, Nimmo HG** (1987) Changes in the kinetic properties and phosphorylation state of phosphoenolpyruvate carboxylase in *Zea mays* leaves in response to light and dark. *FEBS Lett* **213**: 18–22
- Park DH, Somers DE, Kim YS, Choy YH, Lim HK, Soh MS, Kim HJ, Kay SA, Nam HG** (1999) Control of circadian rhythms and photoperiodic flowering by the *Arabidopsis* *GIGANTEA* gene. *Science* **285**: 1579–1582
- Saitou N, Nei M** (1987) The neighbor-joining method: a new method for reconstructing phylogenetic trees. *Mol Biol Evol* **4**: 406–425
- Sambrook J, Fritsch EF, Maniatis T** (1989) *Molecular Cloning: A Laboratory Manual*. Cold Spring Harbor Laboratory Press, Cold Spring Harbor, NY
- Schultz TF, Kiyosue T, Yanovsky M, Wada M, Kay SA** (2001) A role for LKP2 in the circadian clock of *Arabidopsis*. *Plant Cell* **13**: 2659–2670
- Somers DE, Schultz TF, Milnamow M, Kay SA** (2000) *ZEITLUPE* encodes a novel clock-associated PAS protein from *Arabidopsis*. *Cell* **101**: 319–329
- Somers DE, Webb AAR, Pearson M, Kay SA** (1998) The short-period mutant, *toc1-1*, alters circadian clock regulation of multiple outputs throughout development in *Arabidopsis thaliana*. *Development* **125**: 485–494
- Strayer C, Oyama T, Schultz TF, Raman R, Somers DE, Mas P, Panda S, Kreps JA, Kay SA** (2000) Cloning of the *Arabidopsis* clock gene *TOC1*, an autoregulatory response regulator homolog. *Science* **289**: 768–771
- Taybi T, Patil S, Chollet R, Cushman JC** (2000) A minimal serine/threonine protein kinase circadianly regulates phosphoenolpyruvate carboxylase activity in Crassulacean acid metabolism-induced leaves of the common ice plant. *Plant Physiol* **123**: 1471–1481
- Wang Z-Y, Kenigsbuch D, Sun L, Harel E, Ong MS, Tobin EM** (1997) A Myb-related transcription factor is involved in the phytochrome regulation of an *Arabidopsis* *Lhcb* gene. *Plant Cell* **9**: 491–507
- Wang Z-Y, Tobin EM** (1998) Constitutive expression of the CIRCADIAN CLOCK ASSOCIATED1 (CCA1) gene disrupts circadian rhythms and suppresses its own expression. *Cell* **93**: 1207–1217
- Wilkins MB** (1992) Circadian rhythms: their origin and control. *New Phytol* **121**: 347–375
- Wyka TP, Bohn A, Duarte HM, Kaiser F, Lüttge UE** (2004) Perturbations of malate accumulation and the endogenous rhythms of gas exchange in the Crassulacean acid metabolism plant *Kalanchoë daigremontiana*: testing the tonoplast-as-oscillator model. *Planta* **219**: 705–713